Characterization of aspartame–cyclodextrin complexation

Tamás Sohajda[a], Szabolcs Béni[a], Erzsébet Varga[b], Róbert Iványi[b], Ákos Rácz[a], Lajos Szente[b], Béla Noszál[a],*

[a] *Semmelweis University, Department of Pharmaceutical Chemistry, 1092 Budapest, Hőgyes Endre u. 9, Hungary*
[b] *Cyclolab Ltd., 1097 Budapest, Illatos út 7, Hungary*

ABSTRACT

The inclusion complex formation of aspartame (guest) and various cyclodextrins (host) were examined using ^{1}H NMR titration and capillary electrophoresis. Initially the protonation constants of aspartame were determined by NMR-pH titration with *in situ* pH measurement to yield $\log K_1 = 7.83$ and $\log K_2 = 2.96$. Based on these values the stability of the complexes formed by aspartame and 21 different cyclodextrins (CDs) were studied at pH 2.5, pH 5.2 and pH 9.0 values where aspartame exists predominantly in mono-cationic, zwitterionic and monoanionic form, respectively. The host cyclodextrin derivatives differed in various sidechains, degree of substitution, charge and purity so that the effect of these properties could be examined systematically. Concerning size, the seven-membered beta-cyclodextrin and its derivatives have been found to be the most suitable host molecules for complexation. Highest stability was observed for the acetylated derivative with a degree of substitution of 7. The purity of the CD enhanced the complexation while the degree of substitution did not provide obvious consequences. Finally, geometric aspects of the inclusion complex were assessed by 2D ROESY NMR and molecular modelling which proved that the guest's aromatic ring enters the wider end of the host cavity.

© 2009 Elsevier B.V. All rights reserved.

1. Introduction

Cyclodextrins, the drug carrier family of cyclic oligosaccharides are composed of five or more α-D-glucopyranoside units linked 1–4, as in amylose. Typical CDs contain six, seven or eight glucose units and are denoted α-, β- and γ-CDs, respectively [1]. Each of the chiral glucose units is in the rigid chair conformation, which sets the shape of the molecule a hollow truncated cone with O(2)-H and O(3)-H, the secondary hydroxyl groups located on the wider rim, O(6)-H, the primary hydroxyl groups on the narrower rim [2]. The primary hydroxyls on the narrow side of the cavity can rotate, thus partially blocking the cavity, in contrast to the secondary hydroxyls, which are attached by relatively rigid chains and thus cannot rotate. The H-3, H-5 and glucosidic oxygen are located inside the cavity which is relatively hydrophobic, while the other CD protons (H-1, 2, 4, 6) are located outside the CD cavity which is hydrophilic (Fig. 1). As a consequence of these features CDs can encapsulate a variety of hydrophobic molecules, or part of them inside their cavity through non-covalent interactions to form inclusion complexes of host–guest type [2]. A number of chemically modified CDs have been prepared to enhance the inclusion capacity and the physico-chemical properties. The driving forces to form inclusion complexes are electrostatic, van der Waals and hydrophobic interactions as well as hydrogen bonding [3]. Cyclodextrin complexation of pharmaceutical compounds can result in improved properties of the guest, such as solubility, stability, masking of undesirable properties, protection against oxidation, light-induced reaction and loss by evaporation [2,4,5].

A systematic study on a drug–cyclodextrin complexation needs a drug-like guest of 200–500 Da molecular weight, high level of structural flexibility, hydrophobic and hydrogen bonding capacities and changeabilities of charge. Aspartame (*N*-(L-α-aspartyl)-L-phenylalanine-1-methyl ester) (Asm) is a dipeptide of aspartic acid and phenylalanine, used as an artificial, non-saccharide sweetener in the pharmaceutical and food industry (Fig. 1). Depending on its three possible charges, Asm is capable to enter various electrostatic interactions, form hydrophobic and hydrogen bonds, and it can adopt several conformations. The protonation constants of aspartame were determined by Kholeif and Anderegg ($\log K_1 = 7.39$ and $\log K_2 = 3.01$), Scriba et al. ($\log K_1 = 7.87$ and $\log K_2 = 3.04$ (CE), $\log K_2 = 3.19$ (potentiometric titration)) and Maheswaran et al. ($\log K_1 = 7.49$ and $\log K_2 = 3.20$) [6–8].

Until now structure dynamics and stability of some Asm–CD inclusion complexes in acidic medium [7–12] and the effect of complexation to the degradation of the guest in solution [13] have already been studied. The binding constant of Asm–β-CD complex was determined by Garbow et al. ($K = 149.2 \pm 19.7$ at p$D = 4.65$, 30 °C), Moelands et al. ($K = 128$ at pH 4.0, 25 °C), Scriba et al.

* Corresponding author. Tel.: +36 1 4763600x53051; fax: +36 1 2170891.
  E-mail address: nosbel@gytk.sote.hu (B. Noszál).

($K = 42 \pm 4$ at pH 2.5 and $K = 31.5 \pm 4$ at pH 3.5) and Maheswaran et al. ($K = 211 \pm 42$). Moelands et al. have also evaluated the binding constant of HPbCD–Asm ($K = 46$), while Scriba et al. have characterized the DIMEB–Asm complex ($K = 79 \pm 7$ at pH 2.5). The stoichiometry of the inclusion complexes was found to be 1:1 in these studies [8–10]. The structure of similar inclusion complexes were examined with ROESY and molecular modelling by Kahle et al. and Waibel et al., while Maheswaran et al., Garbow et al. and Takahashi et al. studied the structure of Asm–β-CD complex [8,9,14–16]. However, only a few Asm–CD binding constants have so far been reported and all these investigations were in acidic environment. Thus, we carried out our experiments with a long line of CDs at three pH values to find the optimal system for the complexation. Also, our goal was to determine the 3D structure of the complex.

In the first part of this study we examined the protonation equilibria of Asm using ^{1}H NMR-pH titration with *in situ* pH measurement. As indicators we applied chloroacetic acid (ClAc), acetic acid, imidazole and Tris. Monitoring the pH-dependent chemical shift changes the protonation constants of aspartame could be determined.

Concerning the various methods to study inclusion complexation ^{1}H NMR spectroscopy is among the most powerful analytical techniques to quantitate the equilibria between CD and a guest [3]. The stoichiometry and association/binding constant of the host–guest complex can be readily obtained from NMR titration data [17–19]. ^{1}H NMR spectra of mixture of CD and guest molecule are recorded and changes in the chemical shift of both host and guest are studied. The downfield shift of H-3 and H-5 CD cavity protons and upfield shift of aromatic guest protons give clear evidence of the formation of inclusion complex. Sometimes downfield shifts of the guest protons can also be observed.

For the structural information the 2D ROESY NMR technique has been found very helpful to characterize the interaction at atomic level between CD and guest molecule due to the ROE cross peaks between the host and guest protons that get closer than 0.4 nm in space [3,20]. ROESY identifies the moiety of the guest inside the CD cavity and the mode of penetration, i.e. either from narrower or wider rim side, the depth of penetration and orientation of the guest. Besides ROESY, molecular modelling calculations were also carried out to confirm the structure and also, to compare complexation of the guest with different CDs.

Mobility shift affinity capillary electrophoresis (ACE) can be used to determine the host–guest stability constants with CDs, especially for charged guest molecules. The electropherograms of CDs and Asm were recorded and from the mobility changes of Asm and EOF the stability constants could be determined.

Here we report the equilibrium and structural results of our studies on the complexation between 21 cyclodextrins (listed in Table 1) and three differently charged species of aspartame.

2. Materials and methods

2.1. Materials

All native CDs, their derivatives (Table 1) and Asm were the products of Cyclolab (Budapest, Hungary) and they were used without additional purification. H_3BO_3, H_3PO_4, CH_3COOH, NaOH and methanol used for preparation of buffer solutions and chloroacetic acid, acetic acid, imidazole, Tris and HCl used in the determination of the protonation constants were of analytical grade and purchased from the commercial suppliers. The NMR experiments were carried out in H_2O/D_2O 9/1 solution, the D_2O was purchased from Sigma–Aldrich (St. Louis, USA). As an EOF marker in the CE experiments DMSO from Reanal (Budapest, Hungary) and as NMR reference compound in ^{1}H NMR-pH titrations sodium

3-(trimethylsilyl)-1-propanesulfonate (DSS) from Fluka (Buchs, Switzerland) were used. As stabilizer in CE experiments in acidic environment hydroxypropyl-methyl cellulose from Sigma–Aldrich was purchased. Doubly distilled water was used in all experiments.

2.2. Nuclear magnetic resonance procedures (NMR)

All NMR experiments were carried out on a 600 MHz Varian VNMRS spectrometer equipped with a dual 5-mm inverse-detection gradient (IDPFG) probehead in H_2O/D_2O 9/1 or D_2O. ^{1}H chemical shifts were referenced to internal DSS ($\delta = 0.000$ ppm) in case of pH-titrations and internal methanol ($\delta = 3.300$ ppm) in case of CD-titrations. To exclude the significant effect of the interaction between methanol and CDs an additional experiment was carried out in which DSS in D_2O was used as reference in an insert tube. This experiment showed that the effect of CD (10 mM) in the solution on the chemical shift of MeOH was 0.002 ppm, which is negligible in respect of the uncertainty of chemical shift determination (± 0.002 ppm, the same value). Standard pulse sequences and processing routines available in VnmrJ 2.2C/Chempack 4.0 were used with water presaturation. 16–128 scans (depending on the experiment) with a spectral window of 4800 Hz were collected into 32,000 data points, giving a digital resolution of 0.3 Hz/point. The relaxation time was set to 1.5 s using a 6.5 μs 90° pulse at 59 dB. In all experiments, the probe temperature was maintained at 298 K and standard 5 mm NMR tubes were used.

The average extent of penetration and the direction of inclusion were investigated by two-dimensional phase-sensitive rotating frame nuclear Overhauser effect spectroscopy (ROESY). A ROESY experiment is suitable for obtaining information about the spatial proximity of atoms of the host and guest molecules by observing the intermolecular dipolar cross-correlations. The intensities of the cross peaks are proportional to $1/r^6$, where r represents the mean distance between the protons in dipolar interaction. The ROE is a manifestation of cross relaxation between two nonequivalent nuclear spins that are close enough (<5 Å) through space [21]. Intermolecular ROEs between aspartame and cyclodextrin protons directly involved in the host–guest interaction were detected as cross-peaks. The ROESY spectrum was recorded on a (1 mM β-CD, 2 mM Asm, pH* 5.2) sample in D_2O, applying a mixing time of 350 ms during a spin-lock of 2.2 kHz. 256 increments were collected with 32 repetitions and the measured data matrix was processed as a matrix of 4 K (F2) by 1 K (F1) data points.

2.3. Determination of protonation constants (log K)

To acquire a pH-dependent series of ^{1}H NMR spectra, the electrodeless single tube NMR titration was applied [22]. In this method, the whole titration of the guest (3 mM Asm) is carried out in a single NMR tube in H_2O/D_2O 9/1, containing also pH-monitoring indicator molecules. As reference we used DSS ($\delta = 0$ ppm) while chloroacetic acid, acetic acid, imidazole and Tris (2 mM each) served as indicators to provide the accurate pH values between 1.7 and 9.2 [23]. The solution furthermore contained 0.14 M NaCl to set total ionic strength at 0.15 M. As titrants 0.1 M HCl and 0.1 M NaOH were added in small portions (5–20 μl) from a Hamilton syringe and the samples were homogenized afterwards. The pH belonging to each spectrum was calculated from the actual chemical shift of the appropriate indicator (δ_{Ind}^{obs}) using a rearranged form of the Henderson–Hasselbach Eq. (1):

$$\mathrm{pH} = \log K_{Ind} + \frac{\delta_{Ind}^{obs} - \delta_{HInd}}{\delta_{Ind} - \delta_{Ind}^{obs}} \qquad (1)$$

The $\log K_{\text{Ind}}$ indicator protonation constants were determined in separate experiments [23]. The limiting chemical shifts refer to the unprotonated (δ_{Ind}) and protonated (δ_{HInd}) forms of the indicator, respectively. These values are obtained from NMR spectra of sufficiently basic or acidic solutions, respectively. An important criterion of using *in situ* pH indicators is the lack of their interaction with other molecules in the sample. Since the δ_{Ind} and δ_{HInd} values of the same indicator vary from one NMR titration to another within the experimental error (ca. 0.002 ppm), such disturbing interferences are assumed to be negligible [23]. The protonation constants were determined using the chemical shifts of the guest molecule's protons and the actual pH. NMR-pH datasets were evaluated with the OPIUM computer program [24].

2.4. Determination of apparent CD binding constants by NMR titration

The NMR titrations were carried out at pH 5.2 in acetic acid buffer in H_2O/D_2O 9/1 to observe the binding features of the zwitterionic molecules that cannot be determined with CE. An additional NMR titration was performed at pH 9.0 to compare the results of the two methodologies. The samples were equilibrated for 12 h before the experiments. Calibration of NMR spectra was performed by setting the residual methanol signal (3.300 ppm) being a reference without any significant interaction with CDs [25]. Samples of mixtures of CDs and Asm were prepared with molar ratio [CD]/[Asm] ranging from 0.3 to 50. Concentrations of the stock solutions were set to 1 mM for Asm and 10 mM for the CDs. The ionic strength was kept constant at 0.15 M with NaCl.

The NMR shift titration is one of the most common procedures to determine stability constants of inclusion complexes [3]. The observed chemical shifts (δ^{obs}) of the carbon bonded protons of host and guest molecules at various concentration ratios are the weighted average of those of free (δ_{L}) and bound ($\delta_{\text{L-CD}}$) species (2) [26]:

$$\delta^{\text{obs}} = \delta_{\text{L}}\chi_{\text{L}} + \delta_{\text{L-CD}}\chi_{\text{L-CD}} = \frac{\delta_{\text{L}} + \delta_{\text{L-CD}}K_{\text{L-CD}}\,[\text{CD}]}{1 + K_{\text{L-CD}}\,[\text{CD}]} \tag{2}$$

Based on the observed chemical shifts and the concentrations of Asm and CD, the binding constants were calculated with the OPIUM program [24].

2.5. Determination of apparent binding constants by CE

CE experiments were performed on a ^{3D}CE instrument (Agilent Technologies, Waldbronn, Germany), equipped with a photodiode array detector. An untreated fused-silica capillary (50 μm i.d., 375 μm o.d., 64.5 cm total length) from Agilent was used. Conditioning of new capillaries was conducted by flushing with 1 M NaOH for 30 min followed by 0.1 M NaOH and buffer for 10 min each. The capillary cassette temperature was set to 25 °C and the voltage to +30 kV. UV detection was performed at 200, 205, 220 and 225 nm and samples were run in triplicate. Along with the UV traces the current and the voltage were monitored. Between the measurements capillaries were flushed with 0.1 M NaOH, water and the electrophoresis buffer solution without CD for 1 min each.

The running buffers were 0.075 M boric acid/borate at pH 9.0 and 0.05 M phosphoric acid/$H_2PO_4^-$ at pH 2.5 to observe the CD-binding of species Asm^- and $H_2\text{Asm}^+$, respectively. According to kinetic studies, the half-life of Asm in the basic solution is approximately 80 h and in acidic it exceeds 100 days [27]. Each CD was added at various concentrations (5–75 mM) to make up the electrophoresis buffer solutions. The phosphate buffer contained 0.05% (w/w) HPMC to stabilize the solution. The stock Asm solution (3.4 mM) contained 10% (v/v) MeOH and 0.001% (v/v) DMSO, the latter served

as a marker of the electroosmotic flow (EOF). Sample injection occurred at a pressure of 50 mbar for 4 s.

The effective electrophoretic mobility, μ_{eff}, of a charged molecule is a function of the charge-to-size ratio and the viscosity of the electrophoresis media. In practical terms, the effective electrophoretic mobility can be obtained from (3):

$$\mu_{\text{eff}} = \frac{l_c l_{\text{d}}}{U} \times \left(\frac{1}{t} - \frac{1}{t_0} \right) \tag{3}$$

where l_c is the total length of the capillary, l_{d} is the length of the capillary to the detector, U is the applied voltage and t and t_0 are the peak appearance times of the analyte and the EOF, respectively [28]. The presence of additives such as CDs in the electrophoresis buffer changes the viscosity of the media, which, in turn, will affect the effective electrophoretic mobilities (Eq. (3)). The effective mobility of the guest is influenced by the concentration of CD, as Eq. (4) shows:

$$\mu_{\text{eff}} = \frac{\mu_{\text{free}} + \mu_{\text{cplx}}K\,[\text{CD}]}{1 + K\,[\text{CD}]} \tag{4}$$

where μ_{eff} is the ligand effective mobility at the actual CD concentration while μ_{free} and μ_{cplx} are the effective mobility of the free and complexed ligand. Based on Eq. (4), the stability constants were determined using *x*-reciprocal method:

$$\frac{\mu_{\text{eff}} - \mu_{\text{free}}}{[\text{CD}]} = -K(\mu_{\text{eff}} - \mu_{\text{free}}) + K(\mu_{\text{cplx}} - \mu_{\text{free}}) \tag{5}$$

2.6. Molecular modelling

All calculations were performed by the SYBYL program [29]. The initial structures of the cyclodextrins were based on structural data found in the literature [30] and on structures in the Brookhaven Protein Database [31,32]. Optimization applied the MMFF94 s force field [33,34] with 8.0 Å cut-off distance for the non-bonded interactions, 0.7 hydrogen-bond scaling factor and distance dependent dielectric function ($\varepsilon = 78.3$), until 0.01 RMS gradient was reached with the BFGS algorithm. These single structures served as input for the further calculations. The zwitterionic aspartame structures were built by the Biopolymer module of SYBYL, and the conformational space was explored by simulated annealing with a collection of 550 structures. The procedure started at 500 K, the equilibration time was 1 ps. After equilibration, the system was cooled down to 50 K (exponential annealing function was applied). The time for annealing was also 1 ps. The obtained structures were optimized to minima with the same settings as the cyclodextrins. After removal of duplicates and high-energy structures (more than 3 kcal/mol above the lowest energy) a quick Boltzmann-distribution calculation was applied to filter the highest 10% of the low-energy structures. Structures with distances below 6 Å between the C^{15} and the C^4 were rejected. From the remaining 33 structures, the lowest 12 and the highest 6 and additional two random structures were chosen for the complex structure computations. The aspartame conformers were put manually into the cavity of each cyclodextrin with the phenyl rings inside. This orientation of the phenyl ring was suggested by the NMR measurements, and case studies for compounds with similar aromatic rings in the literature [35–38] to preclude bumps and to ensure the highest possible similarity of the initial complexes. The adduct structures were optimized, until 0.1 RMS gradient reached. The calculated energy differences between the sum of the energies of the isolated initial structures and the corresponding complex structures contain the strains of both structures originated from the distortion of the preferable conformations during the complex formation, and the interaction energies for the complexing compounds.
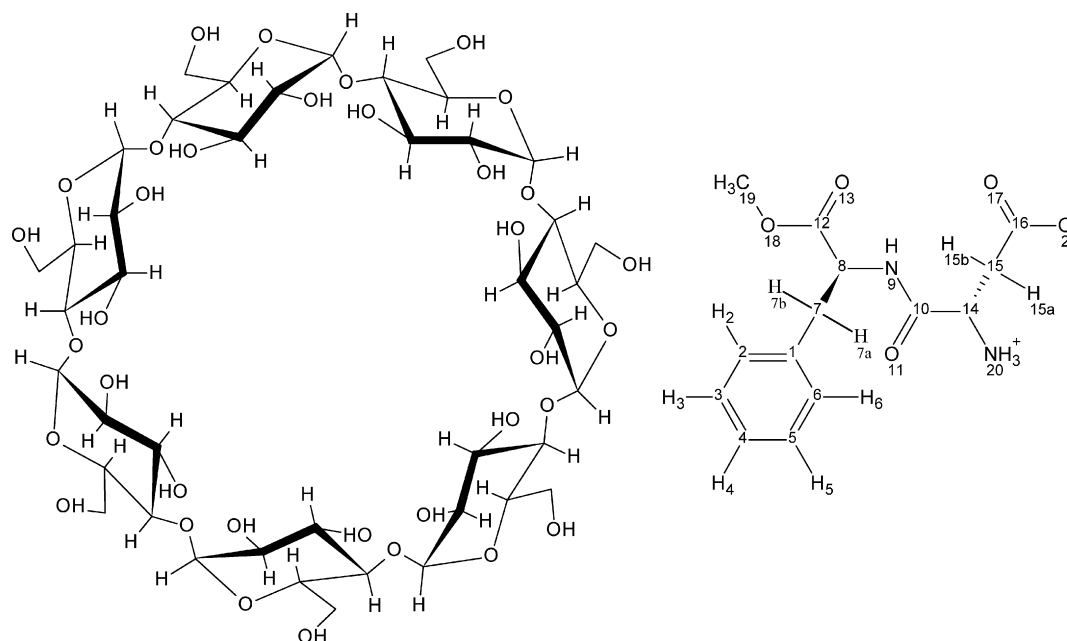
Fig. 1. Chemical structure of the natural β-CD (left) and the zwitterionic form of aspartame (right, with numbering).

3. Results and discussion

3.1. Protonation constants (log K)

The ^{1}H NMR spectra of Asm contain a doublet (H$^{2-6}$) and two triplets (H$^{3-5}$ and H^4) belonging to the aromatic protons near 7.3 ppm. The singlet of the methoxy group (H^{19}) appears at approx. 3.7 ppm, the four doublet–doublets of the methylene groups (H^{7a-b} and H^{15a-b}) between 3.3 and 2.5 ppm and the doublet–doublets of the methine groups near 4.1 (H^{14}) and 4.7 ppm (H^8) at pH 6.5. Numbering of aspartame protons are in superscript, whereas those of CDs are in normal height. The pH-dependent chemical shifts of the H^{14} proton are depicted in Fig. 2.

Since protonation processes are rapid on the NMR time scale, the observed chemical shifts (δ^{obs}) are weighted averages of those of the distinct protonation forms (δ_{Asm^-}, δ_{HAsm}, $\delta_{H_2Asm^+}$):

$$\delta^{obs} = \delta_{Asm^-}\chi_{Asm^-} + \delta_{HAsm}\chi_{HAsm} + \delta_{H_2Asm^+}\chi_{H_2Asm^+}$$

$$= \frac{\delta_{Asm^-} + \delta_{HAsm}K[H^+] + \delta_{H_2Asm^+}K[H^+]^2}{1 + K[H^+] + K[H^+]^2} \quad (6)$$

Expressing the x mole fractions in terms of pH and logarithms of K protonation constants, the master equation to fit the NMR-pH titration curves is obtained (7):

$$\delta^{obs} = \frac{\delta_{Asm^-} + \delta_{HAsm}(10^{\log K_1-pH}) + \delta_{H_2Asm^+}(10^{\log K_1+\log K_2-2pH})}{1 + 10^{\log K_1-pH} + 10^{\log K_1+\log K_2-2pH}}$$

$$(7)$$

The individual chemical shifts (δ_{Asm^-}, δ_{HAsm}, $\delta_{H_2Asm^+}$) and the log K values were calculated from the δ^{obs}-pH datasets (example shown in Fig. 3) with the OPIUM computer program [24].

Not all NMR-pH titration curves exhibit inflections near the log K values. The protonation shifts in ^{1}H NMR spectroscopy are the largest for nuclei in the vicinity of the basic site. Protonation of both the NH$_2$ with log K_1 = 7.83 and the COO$^-$ with log K_2 = 2.96 are monitored most sensitively by the nearby H^{14} methine and H^{15a-b} methylene protons, with chemical shift changes of $\Delta\delta$ 0.623, 0.336 and 0.454 ppm, respectively. The other chain nuclei were also sensitive for the protonation, while the aromatic and methoxy ones were hardly affected. These constants are in good correlation with those of previous papers [6–8].
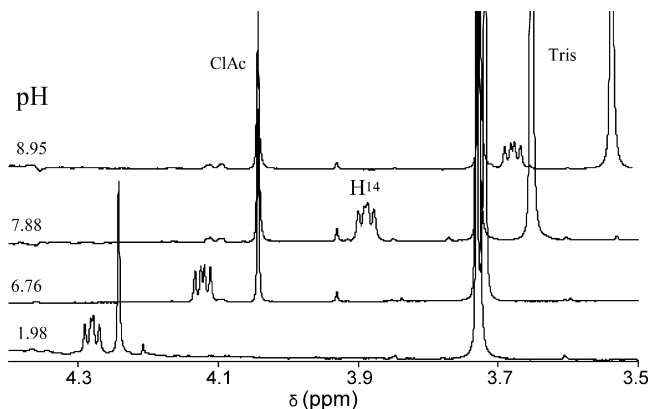

Fig. 2. Representative ^{1}H NMR spectra of the changes of chemical shift in the doublet–doublet of H^{14} Asm at different pH values.
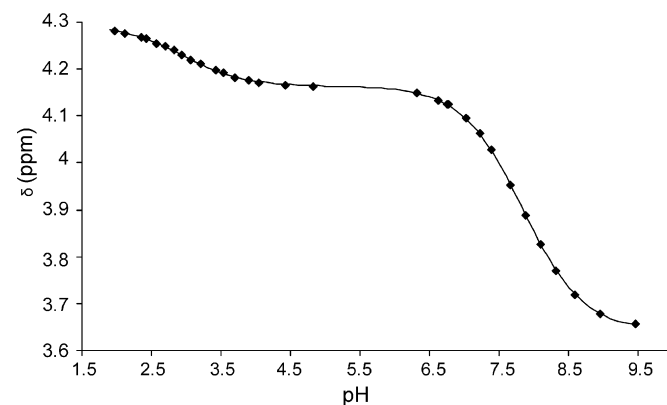

Fig. 3. The titration curve of H^{14} from the ^{1}H NMR-pH titration of aspartame together with curve fitted by OPIUM program.

Table 1
The properties and abbreviations of CD derivatives.

Derivative	Abbreviation	Group(s) attached to the CD	Number of OH group(s) substituted per CD ring	Purity (%)
α-CD	α-CD	(−)	0	100
β-CD	β-CD	(−)	0	100
γ-CD	γ-CD	(−)	0	100
Methylated-β-CD	RAMEB	−CH$_3$	12	>98
Heptakis(2,6-di-O-methyl)-β-CD	DIMEB-95	−CH$_3$	14	>95
Heptakis(2,6-di-O-methyl)-β-CD	DIMEB-98	−CH$_3$	14	>98
Trimethylated-α-CD	TRIMEA	−CH$_3$	18	>98
Trimethylated-β-CD	TRIMEB	−CH$_3$	21	>98
Trimethylated-γ-CD	TRIMEC	−CH$_3$	24	>98
(2-Hydroxy)propyl-β-CD	HPBCD~3	−CH$_2$−CH(OH)−CH$_3$	3 ± 1	>97
(2-Hydroxy)propyl-β-CD	HPBCD~4.5	−CH$_2$−CH(OH)−CH$_3$	4.5 ± 1	>97
(2-Hydroxy)propyl-β-CD	HPBCD~6.3	−CH$_2$−CH(OH)−CH$_3$	6.3 ± 1	>98
Carboxymethylated-β-CD sodium salt	CMBCD	CH$_2$COO$^-$Na$^+$	3 ± 1	>95
Carboxyethylated-β-CD	CEBCD	(CH$_2$)$_2$COOH	3 ± 1	>95
Sulfopropylated-β-CD sodium salt	SPBCD	(CH$_2$)$_3$SO$_3^-$Na$^+$	2 ± 1	>90
6-Monoamino-6-monodeoxy-β-CD	MABCD	−NH$_2$	1	>97
Succinylated-β-CD	SBCD~4	−CO(CH$_2$)$_2$COOH	4 ± 1	>98
Succinylated-β-CD	SBCD~6	−CO(CH$_2$)$_2$COOH	6 ± 1	>95
Acetylated-β-CD	AcBCD~7	−COCH$_3$	7	>95
Acetylated-β-CD	AcBCD~15	−COCH$_3$	15	>95
Phosphated-β-CD sodium salt	PBCD	−PO(OH)O$^-$Na$^+$	2–6	>95

3.2. Binding constants (K)

3.2.1. ^{1}H NMR titrations

^{1}H NMR spectroscopy is the most suitable method for quantification of non-covalent molecular interactions in terms of stability constants ranging from 10 to 10^4 [19]. The incorporation of datasets of several nuclei into the simultaneous evaluation results in more robust estimates of stability constants with smaller error bounds [39]. At the same time, the observed titration shifts ($\Delta\delta$) may provide insight into the structure of the complexes [3]. We carried out experiments at pH 5.2 in acetic acid buffer in which the predominant species is the zwitterionic one (HAsm$_\pm$). All spins of Asm experience chemical shift changes upon complexation. The coupling constants of neither the guests nor the hosts changed in any of the experiments of the determination of protonation or binding constants. Corresponding spectral windows with Asm protons (H$^{15a–b}$, H^{7b}) as a function of cCD/cAsm ratio are shown in Fig. 4.

The CD protons undergo a downfield shift and so do the methylene and methine protons of aspartame, while the aromatic and methyl protons show upfield shifts. A detailed inspection of ^{1}H NMR spectra of mixtures of β-CD and Asm, indicates that the β-CD cavity protons (namely H-3 and H-5) suffer the most significant downfield shifts upon complexation. The concomitant chemical shift changes in the signals of Asm protons in the β-CD–Asm mixtures can only be attributed to the ring current effect of the aromatic ring penetrating the β-CD cavity. This confirms the formation of β-CD–Asm inclusion complex. The most significant changes have surprisingly been observed on the H$^{15a–b}$, H^{7b} and H^{14} protons although the aromatic
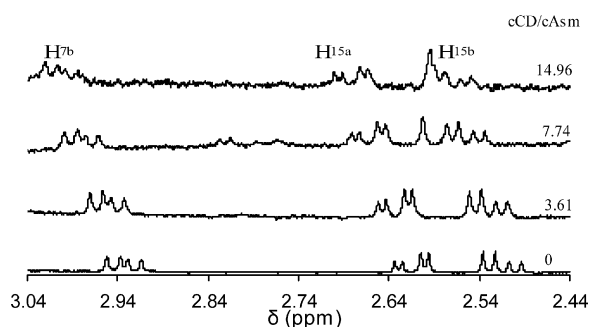
ring was expected to enter the CD ring. The determination of the structure needed therefore further experiments. The triplet of H^8 could not be followed due to its overlap with the remaining peak of the saturated water. Limiting chemical shifts of free and complexed Asm protons in the presence of β-CD are given in Table 2.

The NMR titration curves of nuclei H$^{2–6}$, H$^{3–5}$, H^4, H$^{7a–b}$, H$^{15a–b}$ and H^{19} were included into the simultaneous evaluation according to Eq. (2). The titration curves of two selected Asm nuclei (H$^{3–5}$ and H^{15b}) are shown in Fig. 5. Due to known limitations [19], only the CDs with K higher than 20 could be examined with this method. The evaluated binding constants are collected in Table 3. These data show that most CD derivatives form the most stable complexes with the zwitterionic Asm species.

3.2.2. Capillary electrophoresis

The crucial requirement of application of CE in binding analysis is that at least one of the interacting species has to carry a charge. This is the case for aspartame at pH 2.5 (H$_2$Asm$^+$) and pH 9.0 (Asm$^-$). The mobility of Asm was investigated as a function of the CD concentration in the run buffer. Typical electropherograms of Asm$^-$–β-CD solutions at pH 9.0 are shown in Fig. 6. It is recommended that the analyte concentration should be much smaller than the applied host (CD) concentrations [40], otherwise

Fig. 4. ^{1}H NMR spectra of aspartame H$^{15a–b}$ and H^{7b} at different molar ratios of β-CD and Asm.

Table 2
Limiting chemical shifts of free and complexed Asm and β-CD protons in acetic buffer at pH 5.2 at 25 °C.

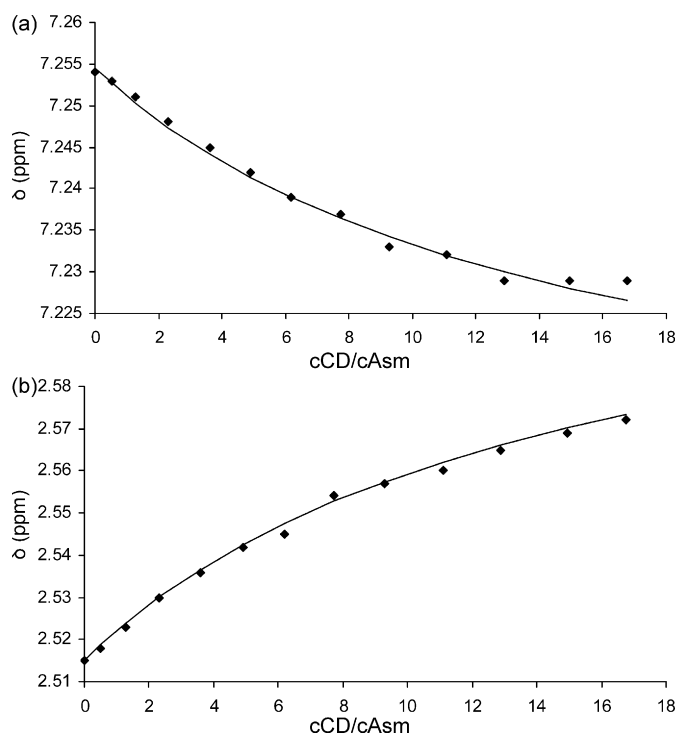| Proton	Free	Complexed
Asm protons		
H$^{2–6}$	7.144	7.120
H$^{3–5}$	7.255	7.202
H^4	7.196	7.180
H^{7a}	3.195	3.210
H^{7b}	2.933	3.074
H^{14}	4.027	4.164
H^{15a}	2.615	2.750
H^{15b}	2.515	2.624
H^{19}	3.596	3.556
CD protons		
H-1	4.928	4.934
H-2	3.512	3.517
H-3	3.881	3.938
H-4	3.710	3.713
H-5	3.599	3.647
H-6	3.826	3.833

Fig. 5. ^{1}H NMR titration curves of (a) H$^{3-5}$ and (b) H^{15b} aspartame protons as functions of host–guest concentration ratio, together with curves fitted by the OPIUM program.
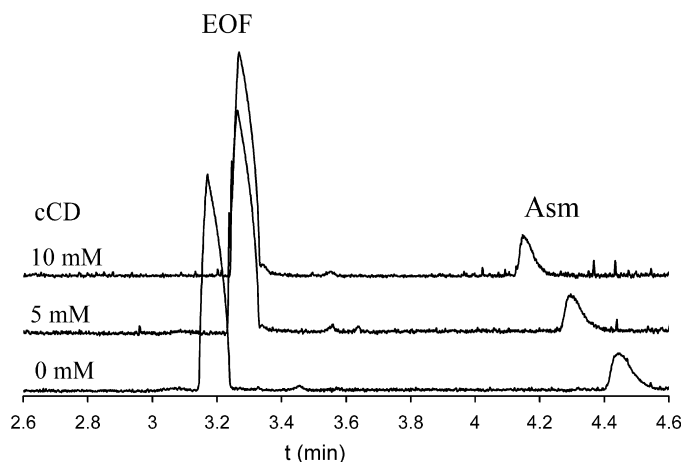

Fig. 6. Representative CE electropherograms of Asm solutions with increasing amounts of CD in the pH 9.0 buffer.

the observed mobility shifts are concentration dependent, reflecting hardly the binding equilibrium. Interaction between Asm and CD is readily apparent in the electropherograms as a shift in Asm peak appearance times relative to the EOF (Fig. 6).

The effective electrophoretic mobilities were calculated according to Eq. (3) from the peak appearance times of the Asm and DMSO, the noninteracting EOF marker. This data as a function of CD concentration was evaluated with a linear curve-fitting method (x-reciprocal). x-Reciprocal plots were linear and the model assuming 1:1 complexation stoichiometry gave realistic binding parameters therefore the 1:1 binding model was accepted. The estimated stability constants ($K_{1:1}$) are compiled in Table 3.

Table 3 shows that the most stable complex of the native CDs is formed with the β-CD. Hence most of the subsequent experiments were carried out with β-CD derivatives. The trimethylation of the native CDs decreased the stability constant for β- and γ-CD but increased it in case of α-CD. The change in the CD structure leads to the extension of the cavity's wider end on H-2, H-3 and H-6 and thus the previously small α-CD fits better opposed to the others. The largest binding constant was determined in the Asm–AcBCD$\sim$7 solutions. The chance for more secondary bonds may explain this outstanding stability. However, further acetylation (AcBCD$\sim$15) provides a steric hindrance and complexation cannot be detected. Concerning the methylated derivatives the purity of the ligand increases the stability of the complex (DIMEB). Rising in the degree of substitution has a less obvious effect among either the methylated or the hydroxypropylated derivatives. The significant stability of the MABCD shows that not only hydrophobic but also ionic bonds promote the complexation. Comparing the differently charged species we may confirm that CDs usually form the most stable complex with zwitterionic aspartame. Determining the binding constant of Asm$^-$–AcBCD$\sim$7 system at pH 9.0 both with CE and NMR titration methods resulted in sufficient agreement (log K = 2.52 vs. log K = 2.75). The difference may be attributed
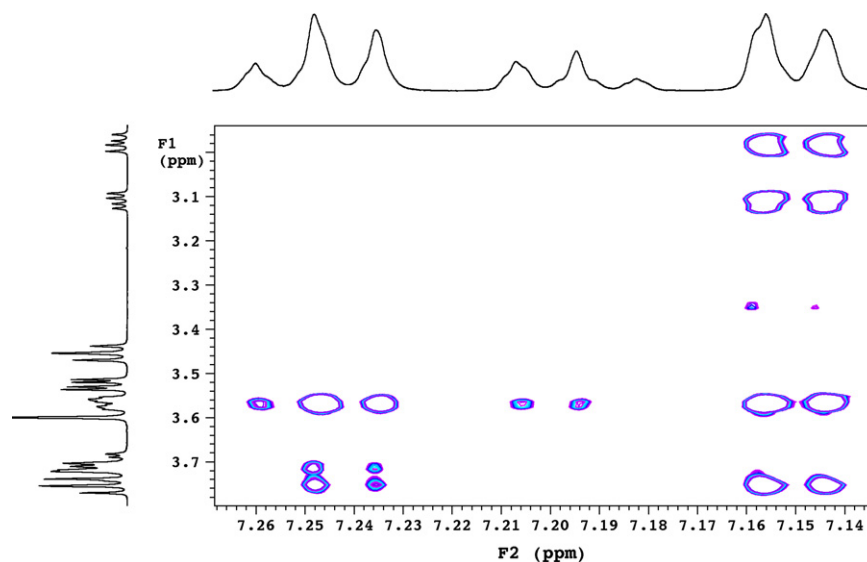
Table 3
The stability constants of Asm–CD complexes determined in this study at 25 °C.

Derivative	K_{Asm^--CD} (obtained with CE)	K_{HAsm^+-CD} (obtained with NMR)	$K_{H_2Asm^+-CD}$ (obtained with CE)
α-CD	8.3 ± 0.4		
β-CD	111 ± 4	123 ± 1	94 ± 2
γ-CD	17.8 ± 0.8		
RAMEB	52.3 ± 5		34.9 ± 6.4
DIMEB-95	41.8 ± 0.9		26.2 ± 4.4
DIMEB-98	61.1 ± 4.1		37.2 ± 8.2
TRIMEA	21.6 ± 0.1	34.1 ± 1.1	
TRIMEB	13.3 ± 1.6		
TRIMEC	3.1 ± 0.2		
HPBCD$\sim$3	68.6 ± 3.3		7.4 ± 1.2
HPBCD$\sim$4.5	20.6 ± 0.4		19.2 ± 7.2
HPBCD$\sim$6.3	45 ± 0.9		26.9 ± 0.6
CMBCD	<10		0
CEBCD	<5		19.1 ± 0.9
SPBCD	10.4 ± 1.4		0
MABCD	94 ± 9	118.6 ± 1.1	82 ± 7
SBCD$\sim$4	0		115 ± 22
SBCD$\sim$6	0		40 ± 10
AcBCD$\sim$7	333 ± 5[a]	253 ± 1	163 ± 17
AcBCD$\sim$15	0		0
PBCD	29.8 ± 8.5		0

[a] The stability constant was determined with ^{1}H NMR titration as well and proved to be 560 ± 2.

Fig. 7. Expansion of the ROESY spectrum (left) of an aqueous sample containing aspartame and β-CD at 2:1 molar ratio.

to the different equilibration times (minutes vs. 12 h), temperature control or the slightly different solvent (H_2O vs. H_2O/D_2O 9/1) in the two methods. Moreover, NMR titration can serve much more reliable stability values as the evaluation of the titration is based on a well-established formula, while the *x*-reciprocal method includes approximations. In acidic and alkaline environment not all the CE experiments could be carried out due to the limited solubility of the CD or the poor stability of the inclusion complex.

3.3. Structure of the inclusion complexes

3.3.1. NMR measurements

The enhanced chemical shift changes shown by H^{2-6}, H^{3-5} and H^4 suggest that the aromatic moiety of aspartame may play a major role in the inclusion process and so does the hydrophobic character of the ring. To verify this hypothesis, 2D ROESY NMR spectra were recorded at pH* 5.2. The expansion of this 2D spectrum in Fig. 7 contains *intramolecular* cross-peaks between H^{7a} (3.1 ppm), H^{7b} (3.0 ppm) and H^{2-6} (7.15 ppm) nuclei of aspartame which belong to the methylene protons adjacent the aromatic ring and the orto-aromatic protons, respectively. From the viewpoint of encapsulation, *intermolecular* cross-peaks of H^{2-6} (7.15 ppm) with the

inner cyclodextrin protons H-5 (3.56 ppm) and H-3 (3.75 ppm) are important. The integral values suggest that the triplet at 7.25 ppm belongs to the meta-protons and the one at 7.19 ppm to the para-proton. Since the cross-peaks of the orto-protons are more intense with the H-3 than those with the H^{3-5} nuclei (7.25 ppm) of the guest, the geometry shown in Fig. 8 can be deduced for the supramolecular complex. Considering that the para-proton only senses the through-space proximity of the H-5 CD proton the inclusion is supposed to proceed through the wider rim of the cyclodextrin. The only intermolecular ROEs observed are between the phenyl ring of aspartame and inner cavity cyclodextrin protons, thus the NMR data clearly suggest a 1:1 stoichiometry for the aspartame-β-CD inclusion complex, which confirms the previous results [8–10,16]. The structure approximation of our ROESY measurements is in good agreement with earlier data as well [8,9,16].

3.3.2. Molecular modelling

The total energy changes of complex formation were −12 to −18 kcal/mol for the β-CD complexes, and −11 to −12 kcal/mol the α-CD complexes. With pairwise comparison of the energy changes of the complexes for each initial aspartame conformer, the differences for the two cyclodextrins were between −0.7 and
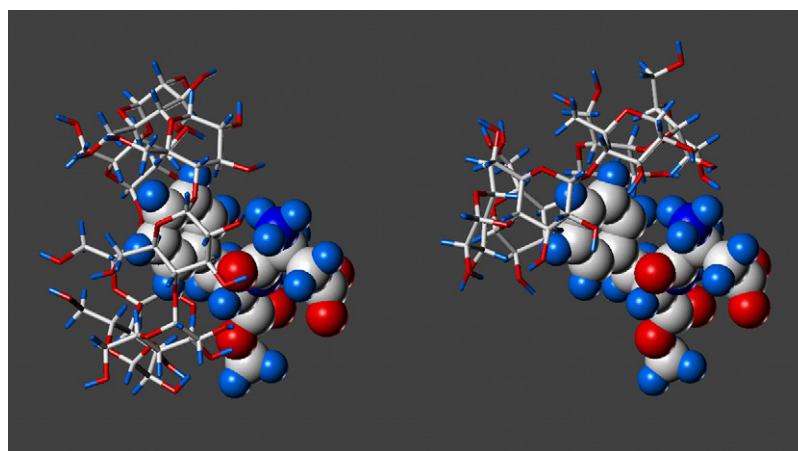

Fig. 8. Representative structure for the aspartame-β-cyclodextrin (left) and aspartame-α-cyclodextrin (right) complexes based on molecular modelling studies and NMR data.

−7.4 kcal/mol with the exception of a 0.3 kcal/mol for one of the twenty conformers (The more negative results mean the preference of the β-CD complex). Most of the differences were within the −3 to −7 kcal/mol range. These energy differences give proper interpretation of the higher stability of the β-CD complexes, which is in good correlation with the experimental observations. The significantly smaller cavity of the α-CD restricts both the entry of the phenyl ring into the CDs inner apolar cavity and prevents the possibility of the hydrogen-bond forming backbone and aspartate side chain to get close enough to the hydroxyl groups on the edge of the cyclodextrin calix. These factors can reduce the attractive interactions between the two molecules, leading concomitantly to the less negative interaction energy. Fig. 8 shows the examples of the complex structures.

4. Conclusion

The interactions of aspartame with various cyclodextrins were characterized in terms of charge-specific complex stability constants. First, the protonation constants of aspartame were determined by NMR-pH titrations with *in situ* pH measurement, after the binding properties were examined at three different pH values with two independent techniques (NMR titration and CE). Our results showed that only a moderately acetylated β-cyclodextrin derivative (AcBCD~7) formed more stable complex with the guest than the parent cyclodextrin. Conclusions of the stability constants are: the complexation depends on the charge of the guest molecule (gross neutral or zwitterionic species are the most appropriate ones), the purity of the CDs improves the stability of the complex (DIMEB-95 vs. DIMEB-98). The effect of the degree of substitution varies with the sidechain, in most cases has a favorable consequence (TRIMEB vs. DIMEB vs. RAMEB or HPBCD~3 vs. ~4.5 vs. ~6.3 in acidic environment). On the basis of ^{1}H NMR complexation shifts and ROESY studies, a geometric model of the supramolecular complex was proposed with the aromatic ring of aspartame and an inclusion through the wider rim of CD. Molecular modelling studies supplied further details, especially on the stability and structural differences between the α-CD and β-CD complexes.

Acknowledgements

References

[1] J. Szejtli, Cyclodextrin Technology, Kluwer Academic Publishers, Dordrecht, 1988.

[2] J. Szejtli, Introduction and general overview of cyclodextrin chemistry, Chem. Rev. 98 (1998) 1743–1753.

[3] H.-J. Schneider, F. Hacket, V. Rudiger, H. Ikeda, NMR studies of cyclodextrins and cyclodextrin complexes, Chem. Rev. 98 (1998) 1755–1785.

[4] T. Loftsson, D. Dûchene, Cyclodextrins and their pharmaceutical applications, Int. J. Pharm. 329 (2007) 1–11.

[5] H.J. Buschmann, D. Knittel, E. Schollmeyer, New textile applications of cyclodextrins, J. Incl. Phenom. 40 (2001) 169–172.

[6] S. Kholeif, G. Anderegg, Equilibrium studies of aspartame and some of its degradation products with hydrogen(I) and copper(II) under physiological conditions using potentiometric pH measurements, Inorg. Chim. Acta 257 (1997) 225–230.

[7] S. Sabbah, F. Suß, G.K.E. Scriba, pH-dependence of complexation constants and complex mobility in capillary electrophoresis separations of dipeptide enantiomers, Electrophoresis 22 (2001) 3163–3170.

[8] M.M. Maheswaran, S. Divakar, Studies on the structure of the inclusion compound of β-cyclodextrin with aspartame, Ind. J. Chem. 30A (1991) 30–34.

[9] J.R. Garbow, J.J. Likos, S.A. Schroeder, Structure, dynamics, and stability of β-cyclodextrin inclusion complexes of aspartame and neotame, J. Agric. Food Chem. 49 (2001) 2053–2060.

[10] D. Moelands, N.A. Karnik, R.J. Prankerd, K.B. Sloan, H.W. Stone, J.H. Perrin, Microcalorimetric study of the interactions of aspartame with β-cyclodextrin and hydroxypropyl-β-cyclodextrin: the anomalous heat of dilution of the latter, Int. J. Pharm. 86 (1992) 263–265.

[11] F. Suß, C.E. Sanger-van de Griend, G.K.E. Scriba, Migration order of dipeptide and tripeptide enantiomers in the presence of single isomer and randomly sulfated cyclodextrins as a function of pH, Electrophoresis 24 (2003) 1069–1076.

[12] S. Sabbah, G.K.E. Scriba, Separation of dipeptide and tripeptide enantiomers in capillary electrophoresis using carboxymethyl-β-cyclodextrin and succinyl-β-cyclodextrin: influence of the amino acid sequence, nature of the cyclodextrin and pH, Electrophoresis 22 (2001) 1385–1393.

[13] R.J. Prankerd, H.W. Soten, K.B. Sloan, J.H. Perrin, Degradation of aspartame in acidic aqueous media and its stabilization by complexation with cyclodextrins or modified cyclodextrins, Int. J. Pharm. 88 (1992) 189–199.

[14] C. Kahle, R. Deubner, C. Schollmayer, J. Scheiber, K. Baumann, U. Holzgrabe, Determination of binding constants of cyclodextrin inclusion complexes with amino acids and dipeptides by potentiometric titration, Chirality 16 (2004) 509–515.

[15] B. Waibel, J. Scheiber, C. Meier, M. Hammitzsch, K. Baumann, G.K.E. Scriba, U. Holzgrabe, Comparison of cyclodextrin-dipeptide inclusion complexes in the absence and presence of urea by means of capillary electrophoresis, nuclear magnetic resonance and molecular modeling, Eur. J. Org. Chem. 18 (2007) 2921–2930.

[16] S. Takahashi, E. Suzuki, Y. Amino, N. Nagashima, Y. Nishimura, M. Tsuboi, Raman and solid state NMR study on an inclusion compound of aspartame with cyclodextrin, Bull. Chem. Soc. Jpn. 59 (1986) 93–96.

[17] B. Chankvetadze, N. Burjanadze, G. Pintore, D. Strickmann, D. Bergenthal, G. Blaschke, Chiral recognition of verapamil by cyclodextrins studied with capillary electrophoresis, NMR spectroscopy, and electrospray ionization mass spectrometry, Chirality 11 (1999) 635–644.

[18] B. Chankvetadze, Combined approach using capillary electrophoresis and NMR spectroscopy for an understanding of enantioselective recognition mechanisms by cyclodextrins, Chem. Soc. Rev. 33 (2004) 337–347.

[19] L. Fielding, Determination of association constants (K_a) from solution NMR data, Tetrahedron 56 (2000) 6151–6170.

[20] D. Neuhaus, M.P. Williamson, The Nuclear Overhauser Effect in Structural and Conformational Analysis, 2nd ed., VCH, Weinheim, 2000.

[21] I. Correia, N. Bezzenine, N. Ronzani, N. Platzer, J.-C. Beloeil, B.-T. Doan, Study of inclusion complexes of acridine with β- and (2,6-di-*O*-methyl)-β-cyclodextrin by use of solubility diagrams and NMR spectroscopy, J. Phys. Org. Chem. 15 (2002) 647–659.

[22] Z. Szakács, G. Hägele, R. Tyka, H-1/P-31 NMR pH indicator series to eliminate the glass electrode in NMR spectroscopic pK(a) determinations, Anal. Chim. Acta 522 (2004) 247–258.

[23] Z. Szakács, Sz. Béni, Z. Varga, L. Őrfi, Gy. Kéri, B. Noszál, Acid–base profiling of imatinib (Gleevec) and its fragments, J. Med. Chem. 48 (2005) 249–255.

[24] M. Kyvala, I. Lukes, OPIUM computer program, 1995, http://www.natur.cuni.cz/~kyvala/opium.html.

[25] G. Tárkányi, Quantitative approach for the screening of cyclodextrins by nuclear magnetic resonance spectroscopy in support of chiral separations in liquid chromatography and capillary electrophoresis; enantioseparation of norgestrel with α-, β- and γ-cyclodextrins, J. Chromatogr. A 961 (2002) 257–276.

[26] H.S. Gutowsky, A. Saika, Dissociation, chemical exchange and the proton magnetic resonance in some aqueous electrolytes, J. Chem. Phys. 21 (1953) 1688–1694.

[27] R.D. Skwierczynksi, K.A. Connors, Demethylation kinetics of aspartame and L-phenylalanine methyl ester in aqueous solution, Pharm. Res. 10 (1993) 1174–1180.

[28] R.A. Wallingford, A.G. Ewing, Capillary electrophoresis, Adv. Chromatogr. 29 (1989) 1–76.

[29] SYBYL® 7.2, Tripos, Inc., 1699 South Hanley Road, St. Louis, MO, USA (2006).

[30] M.M. Pop, K. Goubitz, T. Borodi, M. Bogdan, D.J.A. de Ridder, R. Peshar, H. Schenk, Crystal structure of the inclusion complex of β-cyclodextrin with mefenamic acid from high-resolution synchrotron powder-diffraction data in combination with molecular-mechanics calculations, Acta Crystallogr. B 58 (2002) 1036–1043.

[31] N. Matsumoto, M. Yamada, Y. Kurakata, H. Yoshida, S. Kamitori, A. Nishikawa, T. Tonozuka, Crystal structures of open and closed forms of cyclo/maltodextrin-binding protein, FEBS J. 276 (2009) 3008–3019.

[32] A.K. Schmidt, G.E. Schulz, Structure of cyclodextrin glycosyltransferase complexed with a derivative of its main product beta-cyclodextrin, Biochemistry 37 (1998) 5909–5915.

[33] T.A. Halgren, MMFF VI MMFF94s option for energy minimization studies, J. Comput. Chem. 20 (1999) 720–729.

[34] T.A. Halgren, MMFF VII Characterization of MMFF94, MMFF94s, and other widely available force fields for conformational energies and for intermolecular-interaction energies and geometries, J. Comput. Chem. 20 (1999) 730–748.

[35] V. Thiagarajani, V.K. Indirapriyadharshini, P. Ramamurthy, Fencing of photoinduced electron transfer in nonconjugated bichromophoric system by β-cyclodextrin nanocavity, J. Incl. Phenom. Macro. 56 (2006) 309–313.

[36] S. Anguiano-Igea, F.J. Otero-Espinar, J.L. Vila-Jato, J. Blanco-Mendez, Interaction of clofibrate with cyclodextrin in solution: phase solubility, ^{1}H NMR and molecular modelling studies, Eur. J. Pharm. Sci. 5 (1997) 215–221.

[37] F.J.B. Veiga, C.M. Fernandes, R.A. Carvalho, C.F.G.C. Geraldes, Molecular modelling and 1H-NMR: ultimate tools for the investigation of tolbutamide:

β-cyclodextrin and tolbutamide: hydroxypropyl-β-cyclodextrin complexes, Chem. Pharm. Bull. 49 (2001) 1251–1256.

[38] R.T. Gallagher, C.P. Ball, D.R. Gatehouse, P.J. Bates, M. Lobell, P.J. Derrick, Cyclodextrin-piroxicam inclusion complexes: analyses by mass spectrometry and molecular modeling, Int. J. Mass. Spectrom. Ion Process 165/166 (1997) 523–531.

[39] Sz. Béni, Z. Szakács, O. Csernák, L. Barcza, B. Noszál, Cyclodextrin/imatinib complexation: binding mode and charge dependent stabilities, Eur. J. Pharm. Sci. 30 (2007) 167–174.

[40] S. Bose, J. Yang, D.S. Hage, Guidelines in selecting ligand concentrations for the determination of binding constants by affinity capillary electrophoresis, J. Chromatogr. B 697 (1997) 77–88.